

Article

Magnetic Structure of Inorganic–Organic Hybrid $(\text{C}_6\text{H}_5\text{CH}_2\text{CH}_2\text{NH}_3)_2\text{MnCl}_4$ Using Magnetic Space Group Concept

Garam Park ¹, In-Hwan Oh ^{2,*}, J. M. Sungil Park ³, Seungsoo Hahn ⁴ and Seong-Hun Park ^{5,*}

¹ Nuclear Chemistry Research Team, Korea Atomic Energy Research Institute, Daejeon 34057, Korea; gr860915@kaeri.re.kr

² Quantum Beam Science Division, Korea Atomic Energy Research Institute, Daejeon 34057, Korea

³ Quantum and Convergence Sciences, Korea Atomic Energy Research Institute, Daejeon 34057, Korea; jmspark@kaeri.re.kr

⁴ Da Vinci College of General Education, Chung-Ang University, Seoul 06973, Korea; hahnss@cau.ac.kr

⁵ School of Electrical and Electronics Engineering, College of ICT Engineering, Chun-Aang University, Seoul 06973, Korea

* Correspondence: oh1905@kaeri.re.kr (I.-H.O.); artchem33@naver.com (S.-H.P.)

Received: 29 September 2020; Accepted: 27 November 2020; Published: 30 November 2020



Abstract: Previously, we reported that inorganic–organic hybrid $(\text{C}_6\text{H}_5\text{CH}_2\text{CH}_2\text{NH}_3)_2\text{MnCl}_4$ (Mn-PEA) is antiferromagnetic below 44 K by using magnetic susceptibility and neutron diffraction measurements. Generally, when an antiferromagnetic system is investigated by the neutron diffraction method, half-integer forbidden peaks, which indicate an enlargement of the magnetic cell compared to the chemical cell, should be present. However, in the case of the title compound, integer forbidden peaks are observed, suggesting that the size of the magnetic cell is the same as that of the chemical cell. This phenomenon was until now only theoretically predicted. During our former study, using an irreducible representation method, we suggested that four spin arrangements could be possible candidates and a magnetic cell and chemical cell should coincide. Recently, a magnetic structure analysis employing a magnetic space group has been developed. To confirm our former result by the representation method, in this work we employed a magnetic space group concept, and from this analysis, we show that the magnetic cell must coincide with the nuclear cell because only the Black–White 1 group (equi-translation or same translation group) is possible.

Keywords: inorganic–organic hybrid; magnetic space group; neutron diffraction

1. Introduction

Nowadays, inorganic–organic hybrid materials attract special interest because of their versatile application possibilities, including their use in solar cells, multi-ferroic properties and low-dimensional magnetism [1–4]. To understand interlayer-length effects on their magnetic behavior, many systems have been suggested. Although such trials have taken place, results have not been successful, because inorganic–organic hybrid systems generally show a high insolubility, and it is difficult to obtain a high-quality crystal suitable for a crystallographic investigation. To overcome this hurdle, we have conducted many experiments and finally we have been able to synthesize a series of layered inorganic–organic hybrid perovskite crystals using phenylethylammonium cations. Among others, the crystal structures of $(\text{C}_6\text{H}_5\text{CH}_2\text{CH}_2\text{NH}_3)_2\text{CoCl}_4$ (Co-PEA), $(\text{C}_6\text{H}_5\text{CH}_2\text{CH}_2\text{NH}_3)_2\text{MnCl}_4$ (Mn-PEA) and $(\text{C}_6\text{H}_5\text{CH}_2\text{CH}_2\text{NH}_3)_2\text{CuCl}_4$ (Cu-PEA) have been solved by the X-ray single crystal diffraction technique [5–7]. Co-PEA crystallizes in a monoclinic space group $P12_1/c1$ (No. 14), and shows no magnetic ordering at all at low temperature. Co builds an isolated tetrahedron with Cl and between inorganic and

organic parts various hydrogen bonds exist. Unlike Co-PEA, Mn-PEA and Cu-PEA show an orthorhombic space group $Pbca$ (No.61) and magnetic ordering process occurs at $T_C = 10$ K for Cu-PEA and at $T_N = 44$ K for Mn-PEA. Cu-PEA and Mn-PEA belong to the 2-dimensional layered inorganic–organic K_2NiF_4 perovskite type of general formula A_2MX_4 , where A = organic cation, M = divalent metal and X = halide. Perovskite is the mineral name for $CaTiO_3$. However, in general, ABX_3 or A_2BX_4 type compounds are known as perovskite type. The ABX_3 type is 3-dimensional and A_2BX_4 is a double layered type. The K_2NiF_4 -type materials are also known as Ruddlesden–Popper-type compounds [8]. Although both of the abovementioned Cu-PEA and Mn-PEA are of a magnetically ordered phase below a certain temperature, we prefer Mn-PEA, because Mn-PEA is antiferromagnetic and an antiferromagnetic system is more suitable for handling with neutron diffraction techniques. Additionally, in general, an antiferromagnetic system shows forbidden half-integer peaks below a magnetic transition temperature. However, in the case of Mn-PEA, no half-integer forbidden peaks are observed below the Neel temperature. Instead, integer forbidden peaks that have originated from the magnetic phase transition are present. Based on a theoretical study [9], if weak-ferromagnetism or ferrimagnetism by spin canting due to DM (Dzyaloshinsky-Moriya) interactions is present, the antiferromagnetic cell should be same as the chemical cell. Mn-PEA shows antiferromagnetic phase transition at around 44 K and, in addition, spin canting due to DM interactions causes a weak-ferromagnetism or ferrimagnetism [6]. Thus, this compound should be the ideal candidate material with which the theoretical prediction could be proven. In the previous study, we reported not only X-ray single-crystal structure, but also magnetic properties using magnetic susceptibility and neutron diffraction methods combined with irreducible representation techniques. However, a new approach using a magnetic space group has recently been developed. To check and confirm our previous result using a representation method, in this study, we used a magnetic space group concept, and from this analysis, we will show that the magnetic cell in Mn-PEA is the same as a chemical cell.

2. Materials and Methods

Before we begin, we must first understand what the magnetic moment is and the difference between polar vectors and axial vectors. The magnetic moment of an atom generally refers to spin and is known as an axial vector. A current loop generates a magnetic moment. Under a symmetry operation, a current loop behaves unlike polar vectors such as velocity, force and linear momentum. To describe the axial vector, a new concept of time reversal must be introduced and denoted as $1'$. Under time reversal, the current loop must change its sign and as a result, the spin has to change its direction (see Figure 1).

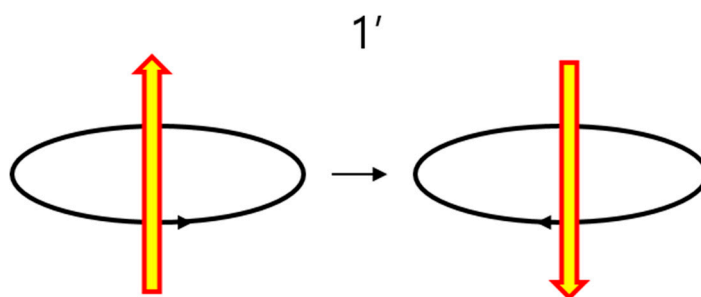


Figure 1. Time reversal effect on the axial vector. The current loop changes its sense under a time-reversal operation.

Contrary to the axial vector, it is unnecessary to consider the loop for a polar vector. Therefore, it is relatively easy to understand the consequences due to the symmetry operation in the case of a polar vector. In Figure 2, the differences between the two vectors under a mirror symmetry operation are shown.

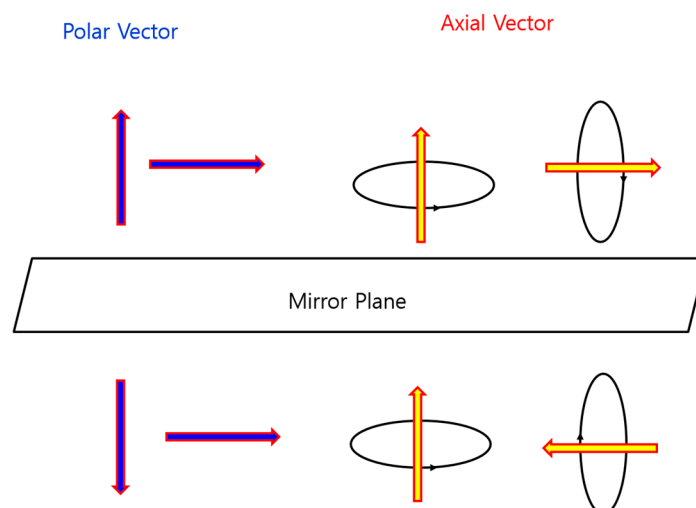


Figure 2. Differences between polar and axial vectors under mirror symmetry operation.

According to the previous study [10], if we denote a magnetic group as M and a conventional crystallographic group as G , all members of G are always a magnetic group. A paramagnetic group is known as a gray group and is described mathematically as $G + G1'$. This means that a paramagnetic group is a simple summation of a crystallographic group and a time reversal applied to crystallographic group $G1'$. The group G is a colorless group. Each colorless group G and paramagnetic group or gray group is composed of 230 groups. The above two groups are trivial. For the magnetic group, the so-called non-trivial Black–White group is important. The Black–White group can be obtained by the coset decomposition technique. Generally, through the coset decomposition method we can obtain many subgroups, but in the case of the magnetic space group, we can only consider subgroups of index 2. This relation is expressed as $M = H + (G - H)1'$, where M is a magnetic group, H is a subgroup of index 2, G is a conventional crystallographic group and $1'$ is a time reversal operation. Using the above relation, we can obtain 1191 Black–White groups. Each group can be divided into two categories based on the existence of translational symmetry changes. According to International Tables for Crystallography A [11], if there is no change in the translational symmetry after the phase transition, the transition is known as *translationengleich* or *t*-transition. This means that the lattice parameters are kept after the phase transition. If there is any change in the translational symmetry, this corresponds to *klassengleich* or *k*-transition. This classical concept is also valid for a magnetic space group, especially for a Black–White group. If we use this concept, there are 674 subgroups that fulfill the equi-transition condition. This group is known as first-kind Black–White, or simply BW1. The subgroup H has the same translation as the parent group G . The last one is a so-called equi-class group or second Black–White group, BW2. In this case, the translation symmetry is lost but the crystal class can be kept [10].

3. Results and Discussion

To analyze the magnetic structure using a magnetic space group concept, we first need information such as space group, lattice parameters and the existence of any phase transitions including structural and magnetic. Mn-PEA has a space group $Pbca$ with lattice parameters $a = 7.207 \text{ \AA}$, $b = 7.301 \text{ \AA}$, $c = 39.413 \text{ \AA}$ and $Z = 4$, and shows two structural and one magnetic phase transitions at 367 K, 417 K and 43 K, respectively [6]. The crystal structure is shown in Figure 3. The point group of the space group $Pbca$ is $2/m2/m2/m$. If we look at the maximal subgroups and minimal super-groups of the point group [11], there are three subgroups with an index 2 of $2/m2/m2/m$, namely, 222 , $mm2$ and $2/m$. In this case, the crystallographic group G is mmm and we can describe the group G as $G_{mmm} = \{1, i, 2, m, 2_x, 2_y, m_x, m_y\}$, where i is inversion symmetry, 2_x is a 2-fold symmetry operation along the x -axis and m_x is a mirror-symmetry operation perpendicular to the x -axis. The possible subgroups

of the mmm point group with index 2 are 222, mm2 and 2/m, as already mentioned above. If we denote one subgroup as H, the first subgroup can be written for example as $H1 = 222 = \{1, 2, 2_x, 2_y\}$. Analogously, we can denote $H2 = mm2 = \{1, m_x, m_y, 2\}$ and $H3 = 2/m = \{1, i, 2, m\}$. In the first case, the magnetic point group $M_{m'm'm'}$ can be obtained from $\{1, 2, 2_x, 2_y\} + \{i, m, m_x, m_y\}1'$ (see Table 1). This is described as $\{1, 2, 2_x, 2_y, i', m', m'_x, m'_y\} = 2'/m'2'/m'2'/m' = m'm'm'$ [10]. This magnetic point group is not compatible with ferromagnetism, because if we look at Table 1, half of the spins have the same sign and the rest of the spins have an opposite sign. This means an antiferromagnetic ordering. Thus, ferromagnetic ordering is impossible in this magnetic point group. This argument is valid for the rest of magnetic point groups. The second one is $\{1, 2, m_x, m_y\} + \{i, m, 2_x, 2_y\}1' = \{1, 2, 2'_x, 2'_y, i, m', m_x, m_y\} = 2'/m2'/m2'/m' = mmm'$ (see Table 1). This magnetic point group is also not compatible with ferromagnetism. In the third case, the corresponding magnetic point group $M_{m'm'2}$ can be obtained from $\{1, 2, i, m\} + \{2_y, m_y, m_x, 2_x\}1'$ (see Table 1). This can be rewritten as $\{1, 2, i, m, 2'_y, m'_y, m'_x, 2'_x\} = 2'/m2'/m2'/m = m'm'2$. This point group is compatible with ferromagnetism. The magnetic point group $m'm'2$ is similar to the previous two magnetic point groups. However, if we consider the magnetic moment along the c-axis, all magnetic components along the c-axis show a positive sign. This means that the ferromagnetic ordering in this point group is only possible along the c-axis. Along another two directions, namely the a- and b-axes, antiferromagnetic ordering is possible. The above results are summarized in Table 1. If the determinant value of the matrix of a symmetry operation is +1, it is known as proper rotation, and if this value is -1, then this is an improper rotation.

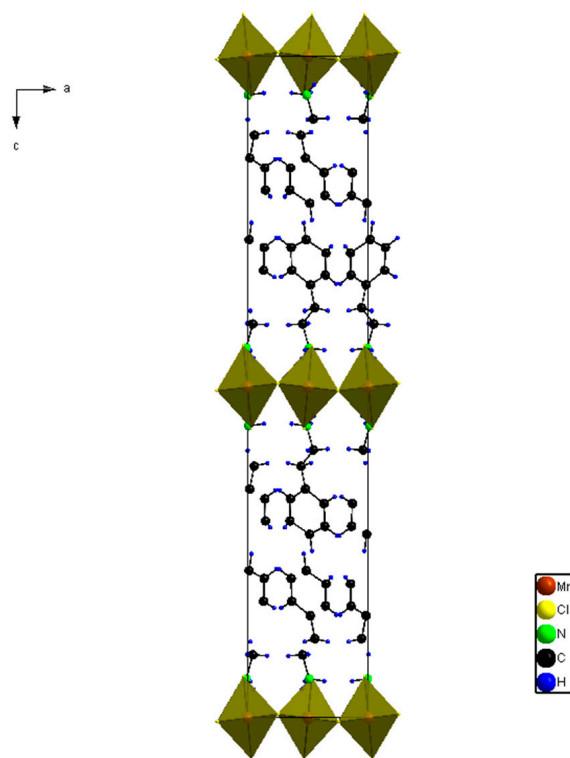


Figure 3. Crystal structure of Mn-PEA at 300 K.

To determine the sign in (x, y, z) form, we have to multiply the determinant of a corresponding symmetry operation by -1 for a primed operation. A primed operation means a symmetry operation combined with the time reversal operation $1'$ [10].

Table 1. Magnetic point groups $M_{m'm'm'}$, $M_{mmmm'}$ and $M_{m'm'2}$. In (x, y, z) form, the integer +1 means a proper rotation and −1 means an improper rotation. m_x , m_y and m_z denote the magnetic components along each axis.

Symbol ($Mm'm'm'$)	(x, y, z) Form	Symbol ($Mmmmm'$)	(x, y, z) Form	Symbol ($Mm'm'2$)	(x, y, z) Form
1	$x, y, z, +1$	1	$x, y, z, +1$	1	$x, y, z, +1$
	m_x, m_y, m_z		m_x, m_y, m_z		m_x, m_y, m_z
2_x	$x, -y, -z, +1$	2_x	$x, -y, -z, +1$	2_z	$-x, -y, z, +1$
	$m_x, -m_y, -m_z$		$m_x, -m_y, -m_z$		$-m_x, -m_y, m_z$
2_y	$x, -y, -z, +1$	m_y	$x, -y, z, +1$	−1	$-x, -y, -z, +1$
	$m_x, -m_y, -m_z$		$-m_x, m_y, -m_z$		m_x, m_y, m_z
2_z	$-x, -y, z, +1$	m_z	$x, y, -z, +1$	m_z	$x, y, -z, +1$
	$-m_x, -m_y, m_z$		$-m_x, -m_y, m_z$		$-m_x, -m_y, m_z$
−1'	$-x, -y, -z, -1$	$2_{y'}$	$-x, -y, -z, -1$	$2_{x'}$	$x, -y, -z, -1$
	$-m_x, -m_y, -m_z$		$-m_x, -m_y, -m_z$		$-m_x, m_y, m_z$
$m_{x'}$	$-x, y, z, -1$	$2_{z'}$	$-x, -y, z, -1$	$2_{y'}$	$-x, y, -z, -1$
	$-m_x, m_y, m_z$		$m_x, m_y, -m_z$		$m_x, -m_y, m_z$
$m_{y'}$	$x, -y, z, -1$	−1'	$-x, -y, -z, -1$	$m_{z'}$	$-x, y, z, -1$
	$m_x, -m_y, m_z$		$-m_x, -m_y, -m_z$		$-m_x, m_y, m_z$
$m_{z'}$	$x, y, -z, -1$	$m_{x'}$	$-x, y, z, -1$	$m_{y'}$	$x, -y, z, -1$
	$m_x, m_y, -m_z$		$-m_x, m_y, m_z$		$m_x, -m_y, m_z$

Now we will check our neutron diffraction experiment data, to find out the most suitable magnetic structure. For neutron diffraction, a large enough single crystal of Mn-PEA was measured on a four-circle diffractometer (Version, Company/Manufacturer, City, State abbrev if USA or Canada, Country) at HANARO, KAERI, Korea. By using a Ge (311) monochromator, a 1.3 Å wavelength was obtained [12,13]. The measurement at low temperature was carried out with closed cycle refrigerator (CCR) (DE-202, ARS, Macungie, PA, USA) and the lowest reachable temperature using CCR was 10 K. In general, the interaction between the neutrons and the nuclei of atoms is isotropic. However, for magnetic scattering, neutrons interact with the electrons in the incompletely filled shells and the intensity from the magnetic scattering shows a strong angle dependency. Besides, neutrons can detect a magnetic moment only if the scattering vector is not parallel to the spin direction. For example, when a magnetic peak is found during a scan process along the a-axis, this indicates that the spin direction is not along the a-axis. To search for magnetic peaks, we used a Q-scan and a radial scan. A propagation vector was obtained through these scans. Down to 10 K, we observed no extra phase transition except magnetic phase transition at around 43 K, which is consistent with previous results from magnetic susceptibility measurements [6]. At room temperature, the space group of Mn-PEA is Pbc_a and the reflection conditions for Pbc_a are as follows: 0kl: $k = 2n$, h0l: $l = 2n$, hk0: $h = 2n$, h00: $h = 2n$, 0k0: $k = 2n$, 00l: $l = 2n$, hkl: $h + k, h + l, k + l = 2n$ and hkl: $h + k, h + l, k + l = 2n$ [11]. This means that above the magnetic phase transition temperature, for example, such as for (1 0 0), (0 1 0) or (0 0 1), reflections are forbidden. If the forbidden peaks are present and also if the intensities of the so-called nuclear peaks remain unchanged, the appearance of a new reflection indicates the beginning of a magnetic phase transition. In addition, if we further cool down the temperature, intensities of magnetic peaks will increase due to the ordering process of a magnetic moment. As shown in Figure 4, below 43 K, new forbidden reflections were observed and based on the nuclear cell, the new reflections were indexed as (−1 0 0), (0 1 0), (1 −2 0) and (3 −3 0) [12]. To check if these peaks were magnetic in origin, we conducted temperature dependence measurements. As shown in Figure 5,

$(-1\ 0\ 0)$ shows a temperature dependency but the intensity of $(2\ 0\ 0)$ is almost constant within an error. To determine the propagation vector, we examined whether we had any half-integer reflections. If any half-integer reflections were observed, it obviously indicated an antiferromagnetic ordering. If not, there are two cases. The first one is a simple ferromagnetic ordering and the second one is an antiferromagnetic ordering. In the antiferromagnetic case, forbidden peaks have to occur. In the title compound, the transition metal Mn, which has a magnetic moment, occupies a special position 4a in the space group $Pbca$ and the former magnetic susceptibility measurement and neutron diffraction experiment indicate that the magnetic moment should be arranged along the c -axis [6,12]. If we look at International Tables for Crystallography A [11], there are three different kinds of maximal non-isomorphic subgroup, namely, I, IIa and IIb, but IIa and IIb are empty. This means that we have to consider only the subgroups belonging to I. All subgroups in I are of index 2 and are composed of seven space groups: $Pbc2_1$, $Pb2_1a$, $P2_1ca$, $P2_12_12_1$, $P112_1/a$, $P12_1/c1$ and $P2_1/b11$. Based on the magnetic space group approach, the magnetic cell must coincide with the nuclear cell, because only the Black–White1 group (type 3, which corresponds to the translationengleich group–maximal non-isomorphic subgroup I) is possible. This means that the propagation vector should be $(0\ 0\ 0)$ and this has already been observed in our previous neutron diffraction experiment [12]. To denote a magnetic space group, two notations are used: Opechowski–Guccione (OG) and Belov–Neronova–Smirnova (BNS). The only difference can be found in the magnetic lattice description and Black–White 2 groups. While BNS notation does not use the primed element in the group symbol, the primed element can be obtained from the magnetic lattice type [14]. Based on the parent space group, we can obtain five possible magnetic space groups: $Pbca$, $Pbca1'$, $Pb'ca$, $Pb'c'a$ and $Pb'c'a'$. The general positions of each magnetic space group are shown in Table 2.

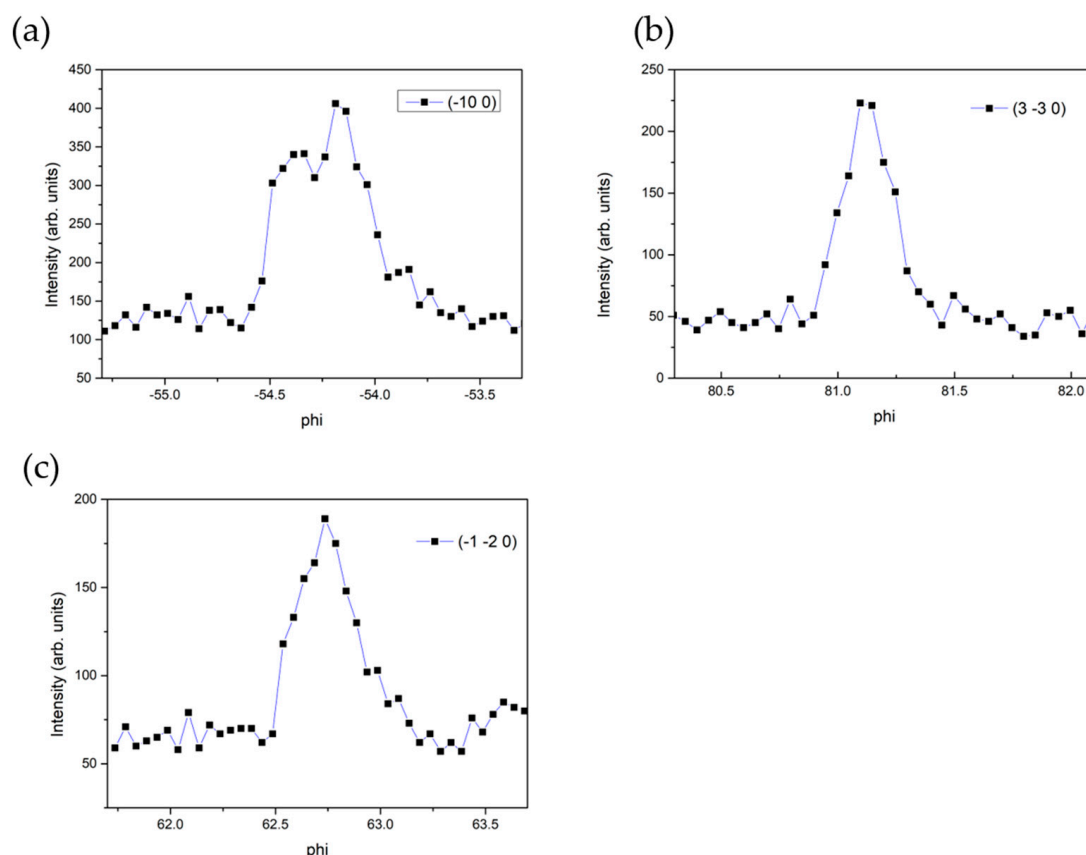


Figure 4. Several selected magnetic peaks below the magnetic phase transition temperature of Mn-PEA [12]. (a) $(-1\ 0\ 0)$; (b) $(3\ -3\ 0)$; (c) $(-1\ -2\ 0)$.

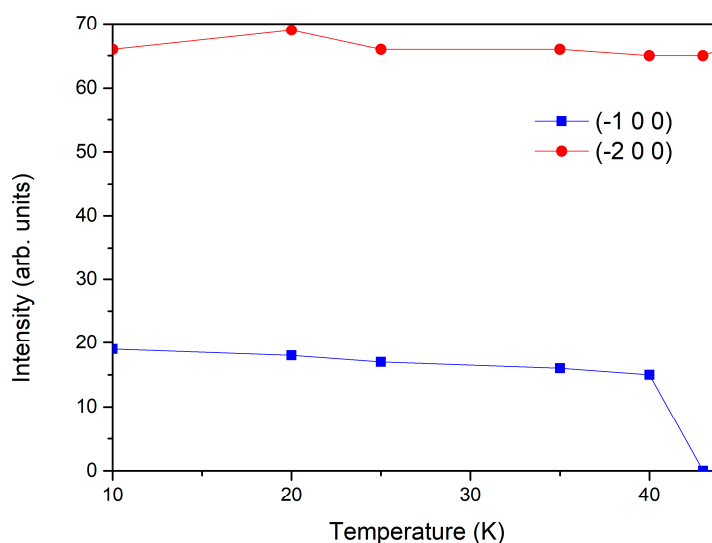


Figure 5. Temperature dependence of forbidden magnetic peak $(-1\ 0\ 0)$ and nuclear peak $(2\ 0\ 0)$ of Mn-PEA from neutron single-crystal diffraction [12].

Table 2. Magnetic space groups $Pbca$, $Pbca1'$, $Pb'ca$, $Pb'c'a$ and $Pb'c'a'$. The integer +1 means a proper rotation and -1 means an improper rotation. m_x , m_y and m_z mean the magnetic component along each axis [15].

$Pbca$	$Pbca1'$	$Pb'ca$	$Pb'c'a$	$Pb'c'a'$
$x, y, z, +1$ m_x, m_y, m_z	$x, y, z, +1$ $0, 0, 0$	$x, y, z, +1$ m_x, m_y, m_z	$x, y, z, +1$ m_x, m_y, m_z	$x, y, z, +1$ m_x, m_y, m_z
$x+1/2, -y+1/2, -z, +1$ $m_x, -m_y, -m_z$	$x+1/2, -y+1/2, -z, +1$ $0, 0, 0$	$x+1/2, -y+1/2, -z, +1$ $m_x, -m_y, -m_z$	$-x+1/2, -y, z+1/2, +1$ $-m_x, -m_y, m_z$	$x+1/2, -y+1/2, -z, +1$ $m_x, -m_y, -m_z$
$-x, y+1/2, -z+1/2, +1$ $-m_x, m_y, -m_z$	$-x, y+1/2, -z+1/2, +1$ $0, 0, 0$	$x, -y+1/2, z+1/2, +1$ $-m_x, m_y, -m_z$	$-x, -y, -z, +1$ m_x, m_y, m_z	$-x, y+1/2, -z+1/2, +1$ $-m_x, m_y, -m_z$
$-x+1/2, -y, z+1/2, +1$ $-m_x, -m_y, m_z$	$-x+1/2, -y, z+1/2, +1$ $0, 0, 0$	$x+1/2, y, -z+1/2, +1$ $-m_x, -m_y, m_z$	$x+1/2, y, -z+1/2, +1$ $-m_x, -m_y, m_z$	$-x+1/2, -y, z+1/2, +1$ $-m_x, -m_y, m_z$
$-x, -y, -z, +1$ m_x, m_y, m_z	$-x, -y, -z, +1$ $0, 0, 0$	$-x, y+1/2, -z+1/2, -1$ $m_x, -m_y, m_z$	$x+1/2, -y+1/2, -z, -1$ $-m_x, m_y, m_z$	$-x, -y, -z, -1$ $-m_x, -m_y, -m_z$
$-x+1/2, y+1/2, z, +1$ $m_x, -m_y, -m_z$	$-x+1/2, y+1/2, z, +1$ $0, 0, 0$	$-x+1/2, -y, z+1/2, -1$ $m_x, m_y, -m_z$	$-x, y+1/2, -z+1/2, -1$ $m_x, -m_y, m_z$	$-x+1/2, y+1/2, z, -1$ $-m_x, m_y, m_z$
$x, -y+1/2, z+1/2, +1$ $-m_x, m_y, -m_z$	$x, -y+1/2, z+1/2, +1$ $0, 0, 0$	$-x, -y, -z, -1$ $-m_x, -m_y, -m_z$	$-x+1/2, y+1/2, z, -1$ $-m_x, m_y, m_z$	$x, -y+1/2, z+1/2, -1$ $m_x, -m_y, m_z$
$x+1/2, y, -z+1/2, +1$ $-m_x, -m_y, m_z$	$x+1/2, y, -z+1/2, +1$ $0, 0, 0$	$-x+1/2, y+1/2, z, -1$ $-m_x, m_y, m_z$	$x, -y+1/2, z+1/2, -1$ $m_x, -m_y, m_z$	$x+1/2, y, -z+1/2, -1$ $m_x, m_y, -m_z$

As already mentioned, the magnetic ion locates on a special position $(0\ 0\ 0)$. If we apply all symmetry operations belonging to the magnetic space group $Pbca$, the final atomic positions are described as follows: $(0, 0, 0 | m_x, m_y, m_z)$, $(1/2, 1/2, 0 | m_x, -m_y, -m_z)$, $(0, 1/2, 1/2 | -m_x, m_y, -m_z)$ and $(1/2, 0, 1/2 | -m_x, -m_y, m_z)$. This magnetic group corresponds to antiferromagnetic ordering. This is shown in Figure 6.

The group $Pbca1'$ in Table 2 is a gray group, which is either paramagnetic or diamagnetic. Therefore, this magnetic group is excluded. This magnetic space group is represented in Figure 7. Because this is para- or diamagnetic, no arrows indicating spins are shown.

In Table 2, the symmetry operations of the magnetic space group $Pb'ca$ are shown. The transition-metal atom Mn locates on $4a$, $(0\ 0\ 0)$. If we apply the magnetic symmetry operations to the Mn atom, we can obtain $\{0, 0, 0 | m_x, m_y, m_z\}$, $\{1/2, 1/2, 0 | m_x, -m_y, -m_z\}$, $\{0, 1/2, 1/2 | -m_x, m_y, -m_z\}$, $\{1/2, 0, 1/2 | -m_x, -m_y, m_z\}$, $\{0, 0, 0 | -m_x, -m_y, -m_z\}$, $\{1/2, 1/2, 0 | -m_x, m_y, m_z\}$, $\{0, 1/2, 1/2 | m_x, -m_y, m_z\}$ and $\{1/2, 0, 1/2 | m_x, m_y, -m_z\}$. For example, the expressions of $\{0, 0, 0 | m_x, m_y, m_z\}$ and

$\{0, 0, 0 | -m_x, -m_y, -m_z\}$ must be same, i.e., $m_x = -m_x$, $m_y = -m_y$ and $m_z = -m_z$. This is also valid for another expression. This means that all magnetic moments must be zero. With this magnetic space group, it is impossible to describe an antiferromagnetic ordering. In Figure 8, the possible spin arrangements are shown.

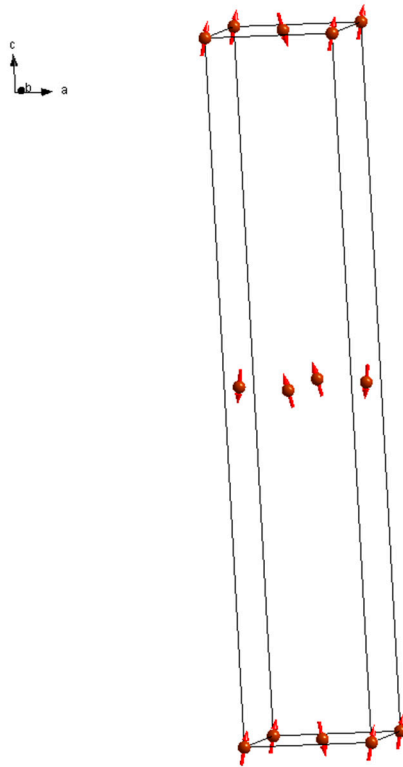


Figure 6. Possible spin arrangement in the magnetic space group Pbc_a .

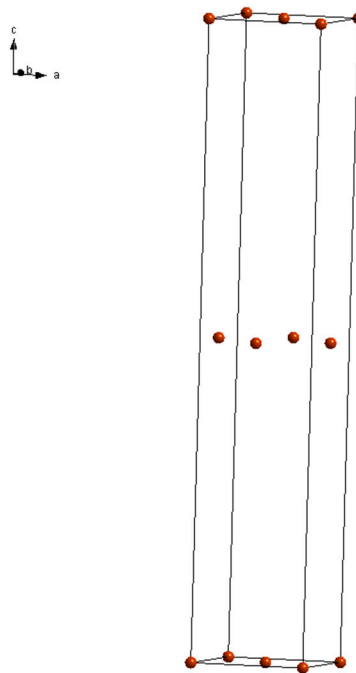


Figure 7. Possible spin arrangement in the magnetic space group Pbc_a1' .

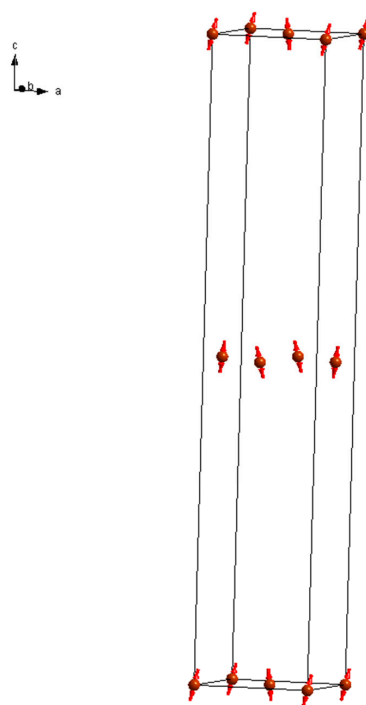


Figure 8. Possible spin arrangement in the magnetic space group $Pb'ca$.

Table 2 shows symmetry operations of the magnetic space group $Pb'ca$. Analogous to the above cases, if we apply all symmetry operations to the Mn atom at $(0\ 0\ 0)$, we obtain $\{0, 0, 0 \mid m_x, m_y, m_z\}$, $\{1/2, 0, 1/2 \mid -m_x, -m_y, m_z\}$, $\{0, 1/2, 1/2 \mid m_x, -m_y, m_z\}$, $\{1/2, 1/2, 0 \mid -m_z, m_y, m_z\}$, $\{0, 0, 0 \mid m_x, m_y, m_z\}$, $\{1/2, 0, 1/2 \mid -m_x, -m_y, m_z\}$, $\{0, 1/2, 1/2 \mid m_x, -m_y, m_z\}$ and $\{1/2, 1/2, 0 \mid -m_x, m_y, m_z\}$. Among a total eight expressions, only four expressions (namely $\{0, 0, 0 \mid m_x, m_y, m_z\}$, $\{1/2, 0, 1/2 \mid -m_x, -m_y, m_z\}$, $\{0, 1/2, 1/2 \mid m_x, -m_y, m_z\}$ and $\{1/2, 1/2, 0 \mid -m_x, m_y, m_z\}$) are unique. Based on this magnetic space group, in the xy -plane, an antiferromagnetic ordering is allowed and along the c -axis, a ferromagnetic ordering is possible. In Figure 9, the spin arrangements of magnetic space group $Pb'ca$ are shown.

In Table 2, the symmetry operations of the magnetic space group $Pb'ca'$ are presented. The transition metal Mn occupies $4a$ $(0, 0, 0)$. As already mentioned, if we apply the magnetic symmetry operations in the magnetic space group $Pb'ca'$ to Mn, we obtain $\{0, 0, 0 \mid m_x, m_y, m_z\}$, $\{1/2, 1/2, 0 \mid m_x, m_y, -m_z\}$, $\{0, 1/2, 1/2 \mid -m_x, m_y, -m_z\}$, $\{1/2, 0, 1/2 \mid -m_x, -m_y, m_z\}$, $\{0, 0, 0 \mid -m_x, -m_y, -m_z\}$, $\{1/2, 1/2, 0 \mid -m_x, m_y, m_z\}$, $\{0, 1/2, 1/2 \mid m_x, -m_y, m_z\}$ and $\{1/2, 0, 1/2 \mid m_x, m_y, -m_z\}$. For example, the expression $\{0, 0, 0 \mid m_x, m_y, m_z\}$ must be equal to $\{0, 0, 0 \mid -m_x, m_y, -m_z\}$ and this means that $m_x = -m_x$, $m_y = -m_y$ and $m_z = -m_z$. To satisfy these conditions, $m_x = m_y = m_z = 0$, i.e., no magnetic ordering is possible if an atom occupies a $4a$ position. In Figure 10, the magnetic space group of $Pb'ca'$ is shown. Among the above five magnetic space groups derived from the crystallographic space group $Pbca$, the magnetic ordering is only possible in the two magnetic space groups $Pbca$ and $Pb'ca$. Compared to the parent crystallographic space group $Pbca$, two magnetic space groups $Pbca$ and $Pb'ca$ show the same translational symmetry, i.e., two magnetic space groups have same lattice parameters of the parent crystallographic space group $Pbca$. This means that the propagation vector must be $(0\ 0\ 0)$. According to the previous research using magnetic susceptibility measurements [6], antiferromagnetic ordering is observed along the c -axis. However, as already discussed in the text, in the case of the magnetic space group $Pb'ca'$, along the c -axis, only ferromagnetic ordering is possible. Thus, the magnetic space group $Pb'ca'$ can be ruled out and the only possible magnetic space group is $Pbca$.

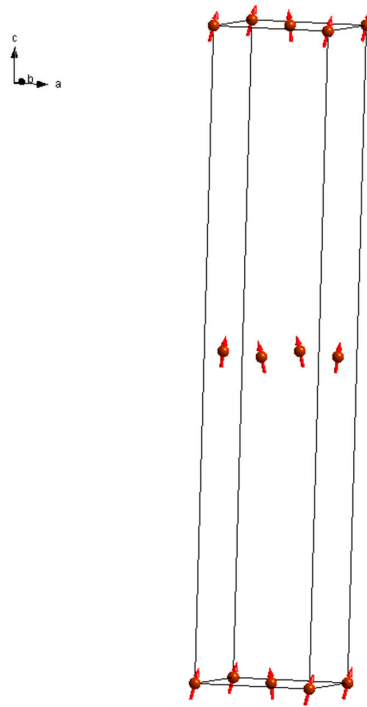


Figure 9. Possible spin arrangement in the magnetic space group $Pb'c'a$. In this configuration, the spin directions of $(0\ 0\ 0)$ and $(1/2\ 1/2\ 0)$ are different. Thus in the xy -plane, antiferromagnetic ordering is possible. This is valid for $(0\ 1/2\ 1/2)$ and $(1/2\ 0\ 1/2)$. Along the c -axis, only ferromagnetic ordering is possible.

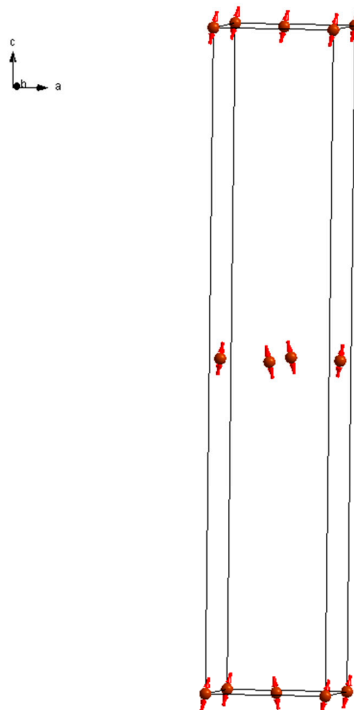


Figure 10. Possible spin arrangement in the magnetic space group $Pb'c'a'$.

4. Conclusions

In our previous works using magnetic susceptibility measurements and neutron diffraction experiments, we claimed that the antiferromagnetic ordering in Mn-PEA is along the c -axis. It was

also shown that the magnetic cell should coincide with the chemical cell. Based on magnetic susceptibility measurements, Mn-PEA has weak-ferromagnetic ordering due to the DM-interaction. Using a neutron diffraction study, we were unable to observe weak ferromagnetism caused by DM-interaction. According to a theoretical study [9], if an antiferromagnetically ordered system shows weak-ferromagnetic ordering due to spin canting, the magnetic and chemical unit cells should be same. Magnetic susceptibility measurements, neutron diffraction, irreducible representation methods and the magnetic space group concept strongly support this hypothesis. During the former neutron diffraction measurements, due to the unexpected defects of the CCR, we were unable to further execute our experiment. In the near future, we plan to conduct a neutron diffraction investigation on Mn-PEA to obtain information on the exact magnetic moment value of Mn^{2+} in the crystal structure, after our reactor is restarted after its long shut-down period.

Author Contributions: Conceptualization, I.-H.O.; neutron experiments, I.-H.O., J.M.S.P.; crystal synthesis, G.P., S.-H.P. and S.H.; writing—original draft preparation, G.P., I.-H.O.; writing—review and editing, I.-H.O. and S.-H.P. All authors have read and agreed to the published version of the manuscript.

Funding: This research was partially funded by the Internal R&D program at KAERI by the Ministry of Science and ICT (MSIT) of the Republic of Korea, 53563-20, 53564-20 and 524220-20 and was also funded by a National Research Foundation Grant by the Ministry of Science and ICT (MSIT) of the Republic of Korea, NRF-2020M2D8A2047959.

Conflicts of Interest: The authors declare no conflict of interest.

References

1. Kagan, C.R.; Mitzi, D.B.; Dimitrakopoulos, C.D. Organic-Inorganic hybrid materials as semiconducting channels in thin-film field-effect transistors. *Science* **1999**, *286*, 945–947. [[CrossRef](#)]
2. Mitzi, D.B. Thin-film deposition of organic-inorganic hybrid materials. *Chem. Comm.* **2001**, *13*, 3283–3298. [[CrossRef](#)]
3. Kundys, B. Multiferroicity and hydrogen ordering in $(C_2H_5NH_3)_2CuCl_4$ featuring dominant ferromagnetic interactions. *Phys. Rev. B* **2010**, *81*, 224434. [[CrossRef](#)]
4. Lines, M.E. Magnetism in two dimensions. *J. Appl. Phys.* **1969**, *40*, 1352–1358. [[CrossRef](#)]
5. Oh, I.H.; Kim, D.; Huh, Y.D.; Park, Y.; Park, J.M.S.; Park, S.H. Bis(2-phenylethylammonium)tetrachloridocobaltate(II). *Acta Cryst. E* **2011**, *67*, m522–m523. [[CrossRef](#)] [[PubMed](#)]
6. Park, S.H.; Oh, I.H.; Park, S.; Park, Y.; Kim, J.H.; Huh, Y.D. Canted antiferromagnetism and spin reorientation transition in layered inorganic-organic perovskite $(C_6H_5CH_2CH_2NH_3)_2MnCl_4$. *Dalton Trans.* **2012**, *41*, 1237–1242. [[CrossRef](#)] [[PubMed](#)]
7. Polyakov, A.O.; Arkenbout, A.H.; Baas, J.; Blake, G.R.; Meetsma, A.; Caretta, A.; van Loosdrecht, P.H.M.; Palstra, T.T.M. Coexisting ferromagnetic and ferroelectric order in a $CuCl_4$ -based organic inorganic hybrid. *Chem. Mater.* **2012**, *24*, 133–139. [[CrossRef](#)]
8. Kim, K.Y.; Park, G.; Cho, J.; Kim, J.; Kim, J.-S.; Jung, J.; Park, K.; You, C.-Y.; Oh, I.H. Intrinsic magnetic order of chemically exfoliated 2D Ruddlesden-Popper organic-inorganic halide perovskite ultrathin films. *Small* **2020**. accepted. [[CrossRef](#)]
9. Izyumov, Y.A.; Ozero, R.P. *Magnetic Neutron Diffraction*; Plenum Press: New York, NY, USA, 1970; pp. 30–31.
10. Aroyo, M.I.; Magnetic Point Groups. Role of Magnetic Symmetry in the Description and Determination of Magnetic Structures. In Proceedings of the IUCr Congress Satellite Workshop, Hamilton, ON, Canada, 14–16 August 2014.
11. Hahn, T. (Ed.) *International Tables for Crystallography*, 5th ed.; Space-Group Symmetry; Kluwer Academic Publishers: Dordrecht, the Netherlands, 2002; Volume A.
12. Park, G.; Oh, I.H.; Park, J.M.S.; Park, S.H.; Hong, C.S.; Lee, K.S. Investigation of magnetic phase transition on the layered inorganic-organic hybrid perovskites $(C_6H_5CH_2CH_2NH_3)_2MnCl_4$ by single-crystal neutron diffraction. *Phys. B Phys. Condens. Matter* **2018**, *561*, 89–93. [[CrossRef](#)]
13. Oh, I.H.; Kim, J.E.; Koo, J.; Park, J.M.S. Refinement of cesium diaquatrichloromanganate(II), $CsMnCl_2 \cdot 2H_2O$ by neutron diffraction, $Cl_3CsH_4MnO_2$. *Z. Kristallogr. NCS* **2014**, *229*, 265–266.

14. Litvin, D.B.; *Magnetic Group Tables. 1-, 2- and 3-Dimensional Magnetic Subperiodic Groups and Magnetic Space Groups. Part 1. Introduction*; International Union of Crystallography: Chester, UK, 2013; Available online: www.iucr.org/publ/978-0-9553602-2-0 (accessed on 30 November 2020).
15. Litvin, D.B.; *Magnetic Group Tables. 1-, 2- and 3-Dimensional Magnetic Subperiodic Groups and Magnetic Space Groups. Part 2. Tables of Magnetic Groups*; International Union of Crystallography: Chester, UK, 2013; Available online: www.iucr.org/publ/978-0-9553602-2-0 (accessed on 30 November 2020).

Publisher’s Note: MDPI stays neutral with regard to jurisdictional claims in published maps and institutional affiliations.



© 2020 by the authors. Licensee MDPI, Basel, Switzerland. This article is an open access article distributed under the terms and conditions of the Creative Commons Attribution (CC BY) license (<http://creativecommons.org/licenses/by/4.0/>).